time t^* characteristic of the statistical passage time of the coherent event minus the rise time of the pulse (which can be neglected at the high Reynolds numbers), a minimum value of the skin-friction coefficient was estimated,[4] (assuming the ideal case where the shear decays lasts until the next pulse occurred). The computed minimum values of $c_{f,\min}$ for the zero-pressure-gradient flow are also shown on Fig. 4. The second-order similarity impulse flow solution[5] includes a term $\phi_1 U' \sqrt{t}$ added to the $1/\sqrt{t}$ term. For an adverse pressure gradient, U' (derivative of the velocity with respect to x) is negative, and so the decay of the surface shear stress will be faster than that for zero-pressure-gradient flow.

The statistical time t^* between the large pulses have been measured for zero-, favorable-, and adverse-pressure-gradient flows.[2,4] Empirical relations to estimate t^* are listed next.

Zero pressure gradient[4]:

$$T^* \equiv U_e \sqrt{t^*/\nu} = 27 + 673 R_\theta \qquad (2)$$

General pressure gradient[2]:

$$\frac{c_{f,\mathrm{mean}}}{f(H, R_\theta)} = 0.170 + 5110(\log T^*)^{-10} \qquad (3)$$

(note that the constants 0.170 and 5110 were inadvertently given as 170 and 5.110×10^{-3} in Ref. 2), where

$$f(H, R_\theta) = \mathcal{S}[1.96 \times 10^{-4} + 8.96 \times 10^{-3} H^{-4}]$$

$$\mathcal{S} = 2.67 - H + \frac{2.45 \times 10^{-5}}{R_\theta} \exp\frac{-(\ln R_\theta - 14)^2}{7.39}$$

$\mathcal{S}$ is an empirical separation criterion, which is zero when $c_{f,\mathrm{mean}} = 0$. The relatons apply for canonical, incompressible, turbulent boundary layers. The lower limit is determined by the laminar-turbulent transition. The upper limit is not known; it appears to apply[4] for $R_\theta > 2 \times 10^5$. An empirical skin-friction relation, which also can predict $c_{f,\mathrm{mean}}$ less than zero:

$$c_{f,\mathrm{mean}} = \mathcal{S}(1.07 H^{-2})\left(R_\theta^{-0.77} - 0.151 R_\theta^{-1.85} + 9.9 \times 10^{-4}\right) \qquad (4)$$

can be used to determine T^* in terms of the mean velocity profile parameters. Modeling of the flow over the time t^* including both the large pulses and the smaller events, such as the streamwise vorticity predicted by large eddy simulation, should lead to a prediction of $c_{f,\mathrm{mean}}$.

IV. Conclusions

Large, time-dependent, surface-shear-stress pulses dominate the surface shear stress for low-Reynolds-number flows, which is the region where most computer modeling studies apply. At higher Reynolds numbers the time between pulses becomes progressively longer, which reduces their contribution to the mean surface shear stress.

The large pulses persist into the adverse pressure regions leading to intermittent separation. The minimum surface shear stress in the turbulent boundary layers appears to be limited by simple viscous decay. The timescale between pulses is a characteristic time related to the production of the surface shear stress in turbulent boundary layers.

References

[1]Jimenez, J., and Moser, R. D., "Large Eddy Simulation: Where Are We and What Can We Expect," *AIAA Journal*, Vol. 38, No. 4, 2000, pp. 605–661.

[2]Sandborn, V. A., "Turbulent Boundary Layer Shear Stress Pulses in Adverse Pressure Gradients," *Proceedings of the 7th AIAA/ASME Joint Thermophysics and Heat Transfer Conference*, edited by B. F. Armaly, HTD-Vol. 357-2, American Society of Mechanical Engineers, New York, 1998, pp. 95–101.

[3]Sandborn, V. A., and Kline, S. J., "Flow Models in Boundary Layer Stall Inception," *Journal of Basic Engineering*, Vol. 83, Series D, No. 3, 1961, pp. 317–327.

[4]Sandborn, V. A., "Surface Shear Stress and Heat Transfer Pulses in Turbulent Boundary Layers," *Turbulence and Shear Flow—1*, edited by S. Banerjee and J. K. Eaton, Begell House, New York, 1999, pp. 1303–1308.

[5]Watson, E. J., "Boundary Layer Growth," *Proceedings of the Royal Society of London, A*, Vol. 231, 1955, pp. 104–116.

J. C. Hermanson
Associate Editor

Influence of the Wall Condition on k–ω Turbulence Model Predictions

Frédéric Thivet,* Mirna Daouk,† and Doyle D. Knight‡
Rutgers University, Piscataway, New Jersey 08854

Introduction

As compared with other two-equation formulations, the k–ω turbulence model[1] seems easier to implement in a numerically robust manner because it does not use any damping function near the walls. However, this formal simplicity is counterbalanced by a high sensitivity of the solutions to the boundary conditions (BC) applied to solve the equations. The sensitivity of the k–ω model to the freestream values of the turbulent quantities is now a well-documented problem,[2,3] which is solved by using two-layer k–ϵ/k–ω formulations[4] for instance. With the wall condition for the turbulent kinetic energy being straightforward ($k_w = 0$), the only questionable BC is the wall condition for ω, which is theoretically infinite at a perfectly smooth wall. Wilcox[1,3] proposes to enforce the asymptotic behavior of ω ($\beta_0 \omega \sim 6\nu_w/y^2$, where $\beta_0 = 0.09$, y is the normal distance to the wall, and ν_w is the molecular viscosity at the wall) on five to seven points above the wall and under $y^+ = 2.5$ [hereafter, the superscript $+$ denotes scaled lengths in wall units: $y^+ = y u_\tau/\nu_w$ with $u_\tau^2 = \nu_w (\partial U/\partial y)_w$ and U is the velocity in the freestream direction]. This very stringent condition, namely the smooth-wall BC for ω, is generally much too expensive to observe in three-dimensional Navier–Stokes computations, so that the alternative is usually to apply the rough-wall BC[1,3]:

$$\omega_w = N \nu_w / k_s^2 \qquad \text{with} \qquad N = 2500 \qquad (1)$$

where k_s is the surface-roughness height. Physically, the flow is insensitive to the roughness height when below five wall units.[5] With such a value the rough-wall condition is expected to be hydrodynamically smooth.[1,3] It is the purpose of this Note to clarify the behavior of the flat-plate boundary-layer solutions obtained with the k–ω model in the range of the hydrodynamically smooth rough-wall BCs for ω.

Numerical Tools

Three numerical codes are used: GASP,[6] EDDYBL,[3] and CLIC2.[7] GASP solves the three-dimensional, compressible, Reynolds-averaged Navier–Stokes equations. The convective fluxes are computed to third-order accuracy using the Roe scheme and the MUSCL reconstruction method with the Min-Mod limiter. The viscous terms are evaluated by second-order central differencing. EDDYBL and CLIC2 solve the compressible, two-dimensional, laminar, transitional, and turbulent boundary-layer equations. Both codes use an adaptive technique to generate the mesh so that the solutions are always fully grid converged. GASP runs the rough-wall BC for ω, EDDYBL the smooth-wall BC, and CLIC2 can run both. In the freestream the turbulent variables are chosen in the range

Received 10 October 2000; revision received 7 July 2001; accepted for publication 8 August 2001.

*Visiting Research Scholar, Department of Mechanical and Aerospace Engineering; permanent position: Senior Research Engineer, Department of Models for Aerodynamics and Energetics, ONERA, 31055 Toulouse, Cedex 4, France. Member AIAA.

†Undergraduate Student, Department of Mechanical and Aerospace Engineering; currently Graduate Student, Department of Aeronautics and Astronautics, Massachusetts Institute of Technology, Cambridge, MA 02139.

‡Professor, Department of Mechanical and Aerospace Engineering. Associate Fellow AIAA.

where the solutions do not depend on them: the ratio of the turbulent to the mean kinetic energy is below 0.1%, and the ratio of the turbulent to the molecular viscosity is 0.001 with GASP and EDDYBL, 0.1 with CLIC2.

Sensitivity of the k–ω Solution to the Roughness Height

The sensitivity of the computed solutions to the value of the roughness height k_s^+ is evaluated in the case of flat-plate boundary layers under two different conditions: 1) Mach number $M_\infty = 4$ and unit Reynolds number $R_u = 26 \times 10^6$ m^{-1}, and 2) $M_\infty = 2$, $R_u = 30 \times 10^6$ m^{-1}. In Fig. 1a the skin-friction coefficient, as obtained in the Mach 4 case with different codes and BCs, is plotted vs R_θ ($R_\theta = R_u\theta$ where θ is the momentum thickness of the boundary layer). The solutions are fully grid converged. The van-Driest II correlation[8] and the smooth-wall solutions obtained with EDDYBL and CLIC2 are given for reference. The inflow condition to each GASP computation is the GASP solution computed before with the rough-wall BC and $k_s^+ = 5$ in a limited region including the flat-plate leading edge. The level of the rough-wall skin friction decreases by about 10% when k_s^+ decreases from 5 to 0.1, which is much more than physically observed.[5]

As expected, when k_s^+ tends toward zero the rough-wall skin-friction coefficient $C_f(k_s^+, R_\theta)$ tends toward a limit, which is very close to both smooth-wall boundary-layer solutions and to the van-Driest II correlation. Therefore it is called the smooth-wall limit $C_{f0}(R_\theta)$. Let $\Delta_r C_f$ be the deviation of the rough-wall skin-friction coefficient from its limit value. Figure 1b shows the behavior of this deviation as obtained for different conditions and solvers when k_s^+ varies. Here again, only fully grid-converged solutions are considered. It is observed that the deviation varies linearly with k_s^+:

$$\Delta_r C_f \equiv \frac{C_f\left(k_s^+, R_\theta\right)}{C_{f0}(R_\theta)} - 1 = \frac{ck_s^+}{100} \tag{2}$$

and that c depends only weakly on the Mach and Reynolds numbers: $c = 1.8 \pm 0.2$.

Equation (2) says that in order to obtain a rough-wall skin-friction coefficient as close as about 1% to the smooth-wall value for instance, the roughness height must be less than 0.5 wall unit. However, the value of k_s^+ must be chosen with care because of the consecutive requirement on the grid, as shown in the following.

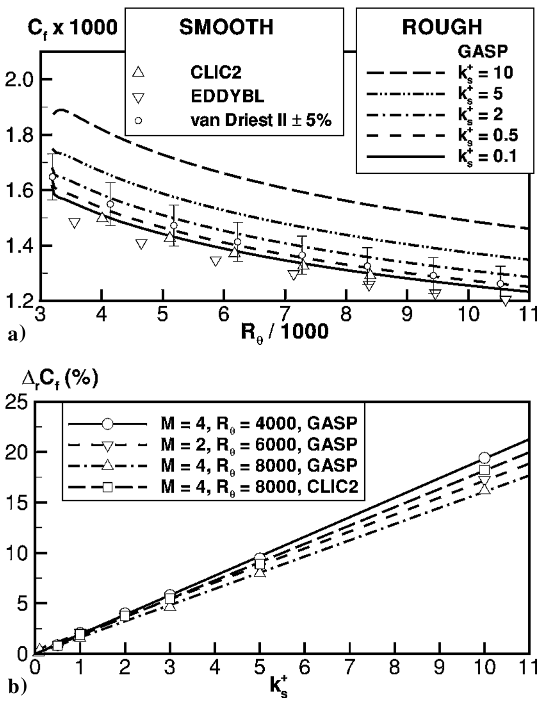

Fig. 1 Behavior of the grid-converged rough-wall skin-friction coefficient: a) effect of the roughness height k_s^+ (Mach 4 case) and b) deviation of the skin-friction coefficient from the smooth-wall value for different conditions and numerical codes.

Condition on the Grid to Avoid Spurious Solutions

For any fixed grid with at least two points in the viscous sublayer, when k_s^+ is lowered from 10 to 0, the skin-friction coefficient decreases according to the linear relationship (2) as long as k_s^+ is above a certain limit. Below this limit, the discrete solution diverges, as illustrated in Fig. 2. The results obtained with GASP on two grids are plotted, each grid having 120 cells inside the boundary layer and a first cell height Δy_1^+ of 0.16 and 0.8 wall unit, respectively. Figure 2 shows that the skin-friction coefficient deviates from the linear behavior when k_s^+ is below about $2\Delta y_1^+$. The same limit is observed on other grids in the range $\Delta y_1^+ = 0.05 - 2$ and for the other considered conditions. Furthermore, Fig. 2 shows that the skin-friction coefficient varies linearly with $\log(k_s^+)$ when k_s^+ is below $2\Delta y_1^+$.

To explain the origin of this boundless departure, Fig. 3 is drawn: here, the profiles of ω are obtained for different values of k_s^+ with GASP on a 120-cell grid with a first cell height of 0.23 wall unit. For reference the smooth-wall EDDYBL solution (circles), the smooth-wall asymptotic behavior (solid line), and the rough-wall asymptotic behaviors [rough-wall: $\beta_0\omega \simeq \omega_w(1 + Cy)^{-2}$ with $\beta_0 C^{-2} = 6\nu_w/\omega_w$] (lines) are also plotted. For each value of k_s^+ above about 0.5, the computed profile of ω (symbols) is very close to the expected asymptotic behavior (lines). However, for values of k_s^+ below 0.5 the computed profiles diverge from the expected asymptotic behavior, and, even worse, values of ω much larger than the smooth-wall limit are obtained. The grid is not fine enough to catch the stiff behavior of ω near the wall, and it results in a significant and boundless decrease of the skin friction. This occurs approximately when k_s^+ is below $2\Delta y_1^+$. The same limit is observed with the boundary-layer code CLIC2 as well. In this case, however, below the limit the computation simply blows up, and no solution can be obtained because of the growth of large instabilities. Consequently,

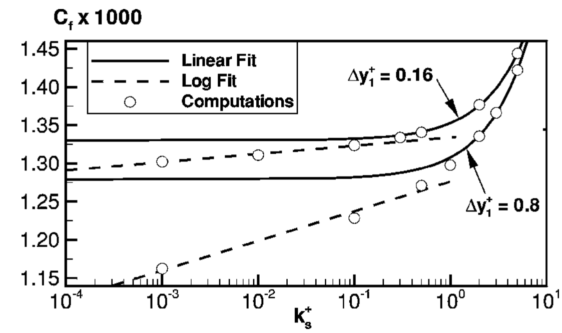

Fig. 2 Evolution of the skin-friction coefficient vs the scaled roughness height k_s^+ on two fixed grids (Mach 4, $R_\theta = 8 \times 10^3$).

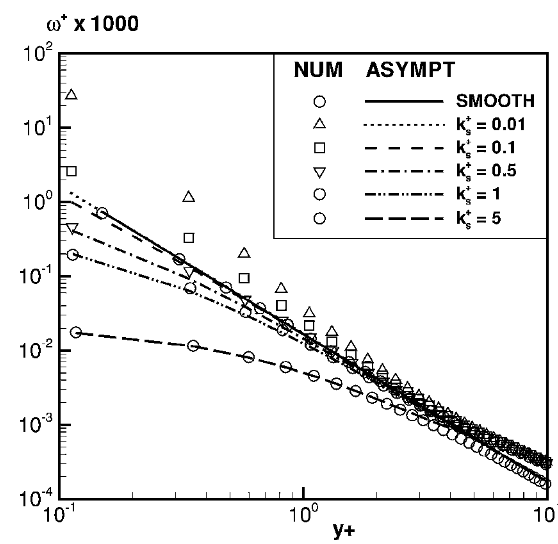

Fig. 3 Profiles of the specific dissipation in the viscous sublayer ($\omega^+ = \nu_w\omega/u_\tau^2$) with different BCs (Mach 4, $R_\theta = 8 \times 10^3$, $\Delta y_1^+ = 0.23$, values reported at the center of the cells).

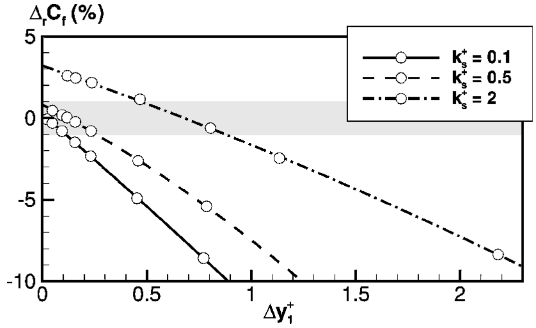

Fig. 4 Deviation of the rough-wall skin-friction coefficient from the smooth-wall value in function of the scaled height of the first cell of the grid (Mach 4, $R_\theta = 8 \times 10^3$).

the limit is the same for two different codes, both based on second-order-accurate numerical schemes. The behavior below this limit is different, with the common point that none of them is desirable.

The preceding section shows that the grid-converged skin-friction coefficient behaves linearly with k_s^+ in the range $k_s^+ = 0 - 10$. This section shows that for a given k_s^+ the height of the first cell off the wall must be at most $k_s^+/2$ in order to avoid a spurious solution. The last question to address is how small the first cell height must be in order to be close to the grid-converged rough-wall solution.

Grid Convergence of the Rough-Wall Boundary-Layer Solution

Figure 4 shows the behavior of deviation (2) for three values of k_s^+ when the grid is refined near the wall. The symbols are the actual results of computations with GASP in the Mach 4 case for $R_\theta = 8 \times 10^3$. The lines are second-order polynomial fits of the computed data. The gray zone represents the range $\pm 1\%$ around the smooth-wall grid-converged value C_{f0}. It is obvious that the smaller k_s^+, the larger the grid-sensitivity of the solution. The values of $C_f(k_s^+)$ reach the limit -1% to C_{f0}, when $\Delta y_1^+ \simeq k_s^+/2$. For k_s^+ below 0.5, the computed solution then stays in the $\pm 1\%$ range when the grid is further refined. However, for k_s^+ above 0.5 (see the case $k_s^+ = 2$ in Fig. 4), the skin-friction value goes on through the $\pm$ 1% range and reaches the significantly different grid-converged value associated with k_s^+. In each case the 1% limit to the grid-converged rough-wall solution is reached when the first cell height is about 0.2.

In Ref. 4 Menter proposes using the following rough-wall BC for ω: $\beta_0 \omega_w = 60 \nu_w / \Delta y_1^2$. This condition is equivalent to the rough-wall BC equation (1) if $k_s = \sqrt{(N\beta_0/60)}\Delta y_1$, which corresponds to a ratio $k_s^+/\Delta y_1^+$ very close to 2 (1.94). As just noted, this relation has the exact effect to keep the solution at the edge $\pm 1\%$ of the smooth-wall value C_{f0} for values of k_s^+ between 0–5 at least: the grid-convergence error compensates for the difference between the rough-wall and the smooth-wall values of the skin-friction coefficient.

Conclusions

The value of the skin-friction coefficient obtained on a flat plate with the $k-\omega$ model and the rough-wall boundary condition for ω is highly sensitive to the scaled roughness height k_s^+. This sensitivity, for k_s^+ below 5, is unphysical. When k_s^+ tends toward zero, the grid-converged computed skin-friction coefficient tends toward the smooth-wall value C_{f0}. The deviation from C_{f0} is directly proportional to k_s^+, with a very weak dependance on the Mach and Reynolds numbers. Namely, $C_f(k_s^+, R_\theta)/C_{f0}(R_\theta) = 1 + (1.8 \pm 0.2)\, k_s^+/100$. This linear relationship is not observed when the grid is too coarse to capture the asymptotic behavior of ω near the wall: with usual second-order numerical methods the first cell height must be smaller than $k_s^+/2$ to avoid spurious or diverged solutions. The observation of the relation $k_s^+/\Delta y_1^+ \simeq 2$ in the range $k_s^+ = 0 - 5$, as recommended by Menter, is sufficient to avoid spurious solutions, but not to get grid convergence. Quite surprisingly, the grid-convergence error in the rough-wall solution yields almost exactly the smooth-wall value of the skin friction. Finally, for the rough-wall skin-friction coefficient to be as close as $x\%$ to the smooth-wall value in a grid-converged way, k_s^+ must be equal to $x/2$, and the first cell height must be below the minimum of 0.2 and $k_s^+/2$.

Acknowledgments

The first author was funded by ONERA and a research fellowship awarded by DGA, the French Armament Procurement Agency, Direction des Systèmes de forces et de la Prospective, under Grant ERE 9960053. The second author was visiting Rutgers University in the framework of an internship from École Polytechnique, supported by the Égide Association from the French Ministry of Foreign Affairs.

References

[1] Wilcox, D. C., "Reassessment of the Scale-Determining Equation for Advanced Turbulence Models," *AIAA Journal*, Vol. 26, No. 11, 1988, pp. 1299–1310.

[2] Menter, F. R., "Influence of Freestream Values on $k-\omega$ Turbulence Model Predictions," *AIAA Journal*, Vol. 30, No. 6, 1992, pp. 1657–1659.

[3] Wilcox, D. C., *Turbulence Modeling for CFD*, 2nd ed., DCW Industries, Inc., La Cañada, CA, 1998, pp. 140–144, 175–177, 343, 344, 461–501.

[4] Menter, F. R., "Two-Equation Eddy-Viscosity Turbulence Models for Engineering Applications," *AIAA Journal*, Vol. 32, No. 8, 1994, pp. 1598–1605.

[5] Nikuradse, J., "Laws of Flows in Rough Pipes," NACA TM 1292, Nov. 1950.

[6] "GASP, General Aerodynamic Simulation Program Version 3," User's Manual, AeroSoft, Inc., Blacksburg, VA, 1996.

[7] Aupoix, B., "Couches Limites Bidimensionnelles Compressibles. Descriptif et Mode d'Emploi du Code CLIC2," ONERA, RF 1/5620.05 DMAE, Toulouse, France, Jan. 1999.

[8] Van Driest, E. R., "Turbulent Boundary Layer in Compressible Fluids," *Journal of Aeronautical Science*, Vol. 18, No. 3, 1951, pp. 145–160.

R. M. C. So
Associate Editor

Turbulent Flow of Power-Law Fluids Through Circular Pipes

Z. U. A. Warsi*
Mississippi State University,
Mississippi State, Mississippi 39762

Nomenclature

a	=	radius of pipe
$F(\tau)$	=	nondimensional $f(t)$
f	=	Fanning friction coefficient for pipes, $\tau_w/\frac{1}{2}\rho\bar{w}_{\text{av}}^2$
$f(t)$	=	pressure gradient, $-\partial\bar{p}/\partial z$
K	=	consistency index
K'	=	$[(3n+1)/4n]^n K$
L	=	section of pipe considered
l	=	l_m/a
l_m	=	turbulent mixing length
n	=	power-law exponent
$\bar{p}$	=	pressure
Q	=	volume flow rate, $\pi a^2 \bar{w}_{\text{av}}$
$R_{e'}$	=	Reynolds number; Eq. (10b)
r	=	radial distance from the centerline
T	=	time used in nondimensionalization
$\bar{T}_{rz}$	=	Reynolds averaged stress component
t	=	time
u_τ	=	friction velocity, $(\tau_w/\rho)^{1/2}$

Received 31 May 2001; revision received 9 October 2001; accepted for publication 9 October 2001.

*Professor of Aerospace Engineering. Associate Fellow AIAA.